

# Application Report

## Understanding Smart Gate Drive



Nicholas Oborny, Ashish Ojha

### ABSTRACT

The gate driver in a motor system design is an integrated circuit (IC) that primarily deals with enhancing external power MOSFETs to drive current to a electric motor. The gate driver acts as an intermediate stage between the logic-level control inputs and the power MOSFETs. The gate driver must be robust and flexible enough to accommodate a wide variety of external MOSFET selections and external system conditions.

Texas Instrument's Smart Gate Drive helps system designers solve a variety of common challenges present in today's motor applications. These challenges include slew rate control and adjustment for optimizing switching and EMC performance, decreasing bill of material (BOM) count, managing MOSFET and system protections, and improving driver timing performance for motor control.

This application report describes the theory and methods behind enhancing a power MOSFET, the various challenges encountered in motor gate driver systems, and the different features implemented in TI Smart Gate Drivers to help solve these challenges.

### Trademarks

All trademarks are the property of their respective owners.

### Table of Contents

<b>1 Power MOSFET Theory and Operation</b>	<b>2</b>
1.1 Basics	2
1.2 Parameters	3
1.3 Turnon Behavior	5
1.4 Simple Slew-Rate Calculation	5
1.4.1 Example	5
1.5 Gate Drive Current	6
1.5.1 Peak Gate Drive Current	6
1.5.2 Average Gate Drive Current	7
<b>2 System Challenges and Smart Gate Drive Features</b>	<b>8</b>
2.1 Slew Rate Control For EMC and Power Loss Optimization	8
2.1.1 System Challenges	8
2.1.2 $I_{DRIVE}$ Implementation	8
2.1.3 $I_{DRIVE}$ Slew Rate Control	9
2.1.4 EMI Optimization Example	12
2.1.5 Slew Time Control	14
2.2 Robust MOSFET Switching Through $T_{DRIVE}$ State Machine	14
2.2.1 MOSFET Handshaking	15
2.2.2 MOSFET Gate-Fault Detection	16
2.2.3 $dV/dt$ Turnon Prevention	17
2.3 System BOM Reduction	18
2.4 Propagation Delay Optimization	20
2.4.1 System Challenges	20
2.4.2 Propagation Delay Reduction	21
<b>3 Revision History</b>	<b>23</b>

# 1 Power MOSFET Theory and Operation

## 1.1 Basics

The metal-oxide-semiconductor field-effect transistor, or MOSFET, is the most common transistor used in present-day electronic-circuit design. The MOSFET has many properties that make it useful in a variety of applications. These properties include scalability, low turnon current, high switching speeds, and high OFF-state impedance. The MOSFET has been used in IC design (analog and digital), switching power applications, motor control, load switches, and numerous other designs.

The MOSFET consists of four terminals which include the drain (D), source (S), gate (G), and body (B) as shown in Figure 1-1. Often, the body terminal is short-circuited to the source terminal making it a three terminal device.

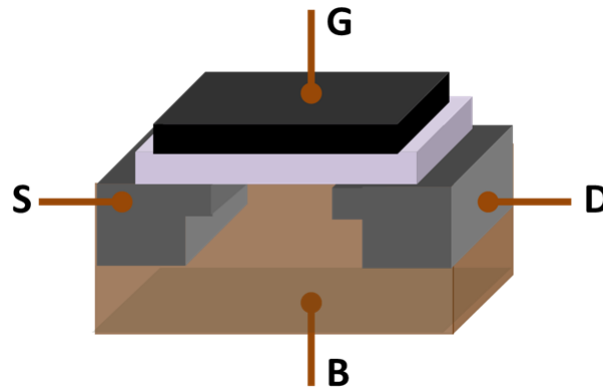


**Figure 1-1. MOSFET Model**

The MOSFET has three basic regions of operation that can be defined with a few simple equations. These regions and their corresponding equations are listed as follows:

- Cutoff

$$V_{GS} \leq V_{th} \quad (1)$$

where

- $V_{GS}$  = Voltage between the gate and source terminals of the MOSFET
- $V_{th}$  = MOSFET threshold voltage

- Linear

$$V_{GS} > V_{th}, V_{DS} \leq V_{GS} - V_{th} \quad (2)$$

where

- $V_{DS}$  = Voltage between the drain and source terminals of the MOSFET

- Saturation

$$V_{GS} > V_{th}, V_{DS} > V_{GS} - V_{th} \quad (3)$$

In the cutoff region, the MOSFET is OFF and no conduction occurs between the drain and the source. In the linear region, the MOSFET is ON and the MOSFET behaves similar to a resistor controlled by the gate voltage with respect to both the source and drain voltages. In the saturation region, the MOSFET is ON and behaves similar to a current source controlled by the drain and gate-to-source voltages.

## 1.2 Parameters

Figure 1-2 shows a common MOSFET model highlighting the terminal-to-terminal capacitances and gate resistance.

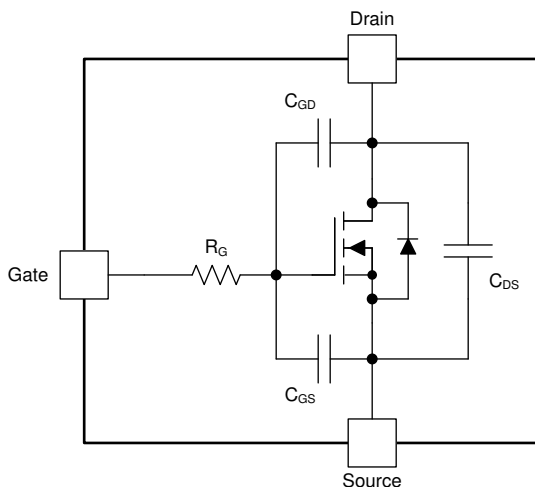


**Figure 1-2. MOSFET Circuit Model**

While the  $C_{GS}$  capacitance is fairly constant, the  $C_{GD}$  and  $C_{DS}$  capacitances vary heavily with the gate-to-drain voltage, drain-to-source voltage, and applied frequency. Table 1-1 lists some typical data sheet parameters of a power-MOSFET. Review these values to understand how they affect the switching performance of the MOSFET.

**Table 1-1. MOSFET Data Sheet Parameters (CSD18532Q5B)**

Parameter	Test Conditions	Min	Typ	Max	Unit
<b>DYNAMIC CHARACTERISTICS</b>					
$C_{iss}$ Input capacitance	$V_{GS} = 0\text{ V}$ , $V_{DS} = 30\text{ V}$ , $f = 1\text{ MHz}$		3900	5070	pF
$C_{oss}$ Output capacitance			470	611	pF
$C_{rss}$ Reverse transfer capacitance			13	17	pF
$R_G$ Series gate resistance			1.2	2.4	$\Omega$
$Q_g$ Gate charge total (10 V)	$V_{DS} = 30\text{ V}$ , $I_D = 25\text{ A}$		44	58	nC
$Q_{gd}$ Gate charge gate-to-drain			6.9		nC
$Q_{gs}$ Gate charge gate-to-source			10		nC
$Q_{g(th)}$ Gate charge at $V_{th}$			6.3		nC
$Q_{oss}$ Output charge	$V_{DS} = 30\text{ V}$ , $V_{GS} = 0\text{ V}$		52		nC
$t_{d(on)}$ Turnon delay time	$V_{DS} = 30\text{ V}$ , $V_{GS} = 10\text{ V}$ , $I_{DS} = 25\text{ A}$ , $R_G = 0\text{ }\Omega$		5.8		ns
$t_r$ Rise time			7.2		ns
$t_{d(off)}$ Turnoff delay time			22		ns
$t_f$ Fall time			3.1		ns

The capacitors and resistor are defined as follows:

**$C_{ISS}$**  A measure of the input capacitance between the gate and source terminals with the drain and source shorted ( $C_{ISS} = C_{GS} + C_{GD}$ ).

**$C_{OSS}$**  A measure of the output capacitance between the drain and source terminals with the gate and source shorted ( $C_{OSS} = C_{DS} + C_{GD}$ ).

**$C_{RSS}$**  The reverse transfer capacitance measured between the drain and gate terminals with the source connected to ground ( $C_{RSS} = C_{GD}$ ).

**$R_G$**  The series resistance in line with the gate terminal.

To account for variation in the capacitance value with respect to voltage, a gate charge curve is typically used to provide more meaningful information. Gate charge values relate to the charge stored within the inter-terminal capacitances. Gate charge is more useful for system designers because it takes into account the changes in capacitance with respect to voltage during a switching transient.

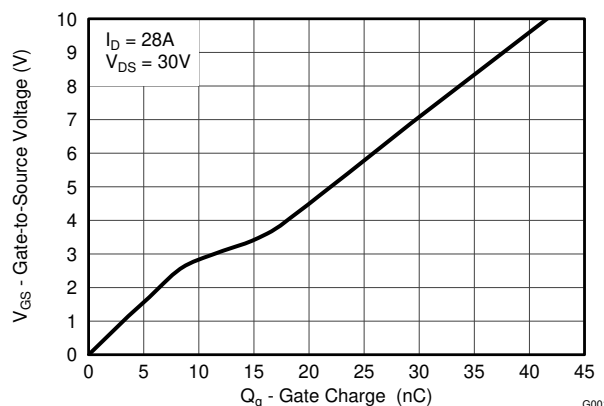


**Figure 1-3. MOSFET Gate-Charge Curve**

The gate charge parameters are defined as follows:

- Q<sub>G</sub>** The total gate charge required to raise the gate-to-source voltage to the specified value (4.5 V and 10 V are commonly used voltages).
- Q<sub>G(th)</sub>** The charge required from 0 V to the threshold voltage of the MOSFET. Current will start to flow from the drain to the source at the threshold voltage.
- Q<sub>GS</sub>** The charge required from 0 V to the Miller plateau voltage. At the plateau voltage the drain to source voltage will start to slew.
- Q<sub>GD</sub>** The charge required to move through the Miller region. The Miller region derives its name from the fact that the gate-to-source voltage stays relatively constant during this period as the reverse transfer capacitance is charged. The MOSFET  $V_{DS}$  slew occurs during this period as the MOSFET becomes enhanced.

#### Note

It should be noted that both  $Q_{GD}$  and in turn  $Q_G$ , while improved figures of merit for MOSFET switching versus capacitance, still have a dependency on  $V_{DS}$  and this should be factored when utilizing these parameters.

## 1.3 Turnon Behavior

Based on the information provided in [Section 1.2](#), a specific amount of charge is required to bias the gate to a certain voltage. With this understanding, how the MOSFET behaves when certain voltages and currents are applied to it starts to become clearer. [Figure 1-4](#) shows the typical turnon response of a MOSFET.

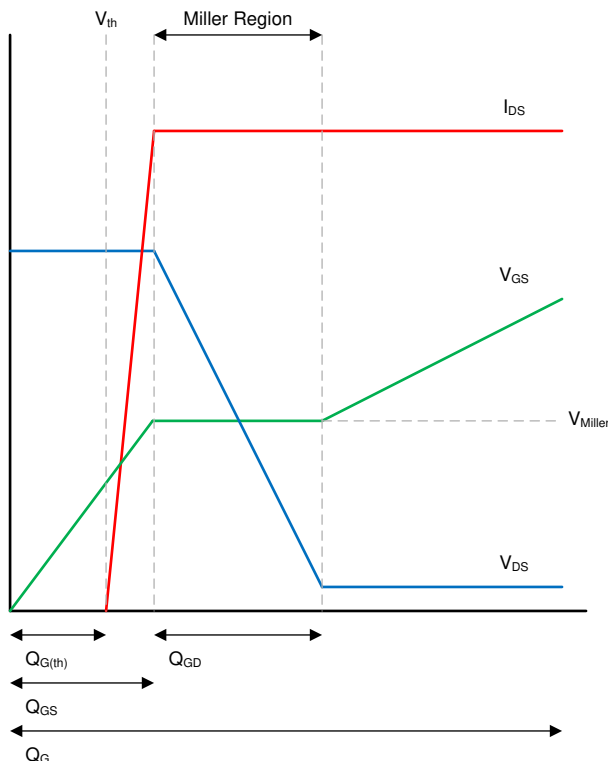


**Figure 1-4. MOSFET Turnon Response**

The curve starts with the gate-to-source voltage increasing as a charge is supplied to the gate. When the gate-to-source voltage reaches the MOSFET threshold voltage, current starts to flow from the drain to the source. The gate-to-source voltage then stays fairly steady as the MOSFET moves through the Miller region. During the Miller region, the drain-to-source voltage drops. After the Miller region, the gate continues to charge until it reaches the final drive voltage.

## 1.4 Simple Slew-Rate Calculation

Unfortunately, calculating precise MOSFET  $V_{DS}$  slew rates from parameters and equations requires specific knowledge of the MOSFET, the board and package parasitics, and detailed information on the gate drive circuit. These calculations go beyond the scope of this document. This document just focuses on simple first order approximations that are compared to lab data.

Because the MOSFET  $V_{DS}$  slew occurs during the Miller region, the Miller charge ( $Q_{GD}$ ) and gate drive strength can be used to approximate the slew rate. The first assumption that should be made is that an ideal, or close to ideal, constant-current source is being used for the MOSFET gate drive.

### 1.4.1 Example

[Figure 1-5](#) shows a [DRV8701](#) Smart Gate Driver driving a CSD18532Q5B at 24 V. The DRV8701 device is configured for the 25-mA source-current setting. The waveform shows an approximately 312-ns slew rate which matches closely with the first order approximation calculated using [Equation 4](#).

$$t_{\text{SLEW}} = \frac{Q_{\text{GD}}}{I_{\text{SOURCE}}}$$

$$t_{\text{SLEW}} = \frac{6.9 \text{ nC}}{25 \text{ mA}} = 276 \text{ ns} \quad (4)$$

where

- $Q_{\text{GD}} = 6.9 \text{ nC}$
- $I_{\text{SOURCE}} = 25 \text{ mA}$

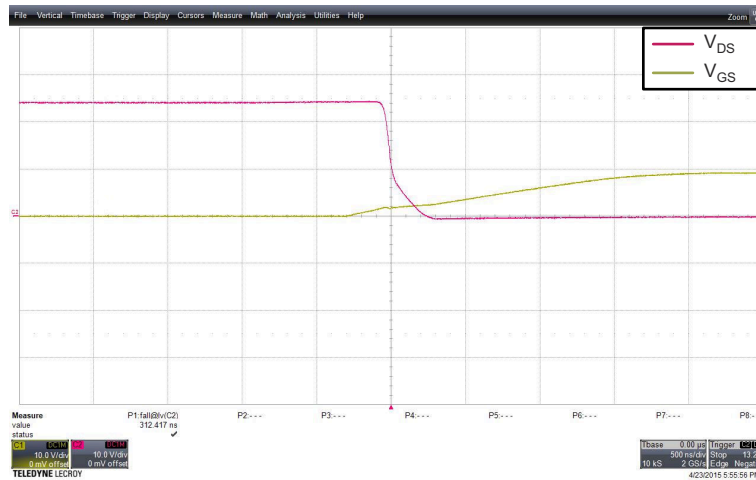


**Figure 1-5. Measured MOSFET Slew Rate**

## 1.5 Gate Drive Current

Peak gate drive current and average gate drive current are two key parameters that should be examined when designing a switching power-MOSFET system, such as a motor drive.

### 1.5.1 Peak Gate Drive Current

The peak gate drive current is the peak current that the gate driver can source or sink to the power MOSFET gate during the turnon and turnoff periods. This value is primarily responsible for how fast the MOSFET can slew.

#### 1.5.1.1 Example

The DRV8701 supports a peak source current of 150 mA and a peak sink current of 300 mA. Using the example from [Section 1.4.1](#), a rise and fall time can be calculated using [Equation 5](#) and [Equation 6](#) (respectively).

$$t_{\text{RISE}} = \frac{Q_{\text{GD}}}{I_{\text{SOURCE}}}$$

$$t_{\text{RISE}} = \frac{6.9 \text{ nC}}{150 \text{ mA}} = 46 \text{ ns} \quad (5)$$

where

- $Q_{\text{GD}} = 6.9 \text{ nC}$
- $I_{\text{SOURCE}} = 150 \text{ mA}$

$$t_{\text{FALL}} = \frac{Q_{\text{GD}}}{I_{\text{Sink}}}$$

$$t_{\text{FALL}} = \frac{6.9 \text{ nC}}{300 \text{ mA}} = 23 \text{ ns} \quad (6)$$

where

- $Q_{\text{GD}} = 6.9 \text{ nC}$
- $I_{\text{SINK}} = 300 \text{ mA}$

### 1.5.2 Average Gate Drive Current

The average gate drive current is the average current required from the gate driver when switching the power MOSFETs constantly. As previously described, the amount of charge to switch a power MOSFET is small (44 nC), but when switching the MOSFET in the kHz range, this charge will average into a constant current draw from the gate driver supply.

Use [Equation 7](#) to calculate the average gate drive current.

$$I_{\text{AVG}} = Q_{\text{G}} * \# \text{ MOSFETs Switching} * \text{Switching Frequency} \quad (7)$$

#### 1.5.2.1 Example

$$I_{\text{AVG}} = 44 \text{ nC} * 6 * 45 \text{ kHz} = 11.88 \text{ mA} \quad (8)$$

## 2 System Challenges and Smart Gate Drive Features

This section describes the various challenges encountered in motor gate driver systems and the different features implemented in TI Smart Gate Drivers to help solve these challenges.

### 2.1 Slew Rate Control For EMC and Power Loss Optimization

#### 2.1.1 System Challenges

Adjustment and tuning of the MOSFET  $V_{DS}$  slew rate is often the first and most critical challenge faced in motor gate driver system design. The MOSFET slew rate directly impacts multiple performance parameters including but not limited to switching power dissipation, radiated emissions, diode recovery and inductive voltage spikes, and  $dV/dt$  parasitic turnon.

While oftentimes there are multiple methods to tackle these challenges (a topic outside the scope of this paper), a common variable they all share is a direct dependency on slew rate. Typically the main tradeoff to consider is that slower slew rates improve performance in radiated emissions, voltage spikes, and parasitic coupling, but will increase power dissipation. Finding the proper balance for this tradeoff is a consideration for every motor system designer.

For further understanding on slew rate and its various impacts to MOSFET performance, you can find further reading in these papers.

- [Fundamentals of MOSFET and IGBT Gate Driver Circuits](#)
- [Optimizing MOSFET Characteristics by Adjusting Gate Drive Amplitude](#)
- [Reduce buck-converter EMI and voltage stress by minimizing inductive parasitics](#)

#### 2.1.2 $I_{DRIVE}$ Implementation

As described earlier, precisely controlling the current applied to the MOSFET gate lets the user make a reasonable calculation for and adjust the MOSFET  $V_{DS}$  slew rate. Texas Instruments Smart Gate Drivers incorporate an adjustable gate drive current scheme in many of the motor gate drivers to easily control the MOSFET slew rate. The adjustable gate drive current parameter is called  $I_{DRIVE}$ . This section describes how  $I_{DRIVE}$  is commonly setup and implemented.

The most commonly implemented method is shown in [Figure 2-1](#). In this method, a MOSFET predriver switch is enabled between the gate and the voltage supply to manage the current directed to the external power MOSFET gate.

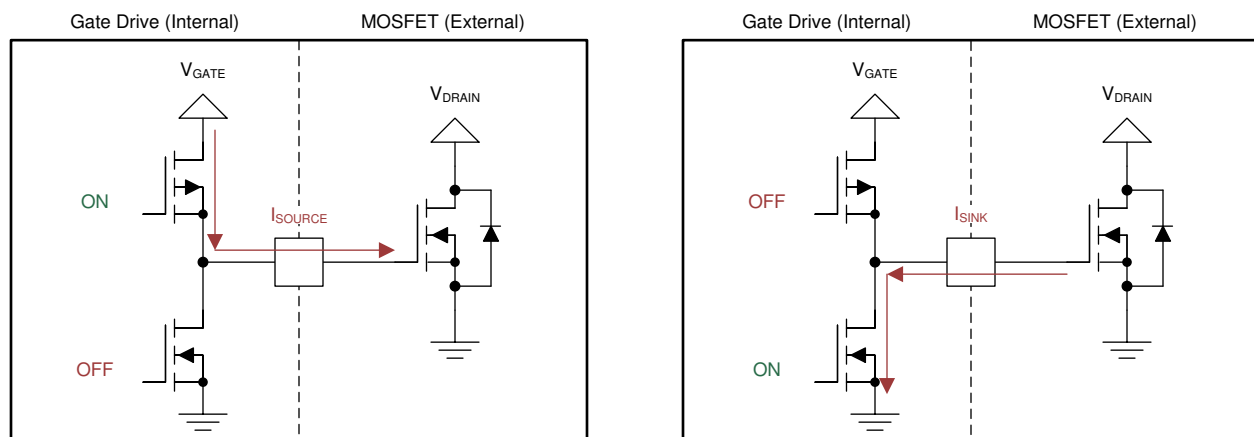


**Figure 2-1. Switch  $I_{DRIVE}$  Method**

To control the current to the gate of the external MOSFET during the  $V_{DS}$  slew, the Smart Gate Driver takes advantage of several MOSFET properties. If the switch (predriver MOSFET) can be operated in the saturation region ([Section 1.1](#)), the current to the external MOSFET is limited to a fixed value. As the external MOSFET moves through the Miller region, the gate-to-source voltage plateaus and stays relatively constant ([Section 1.3](#)).

Using these two properties, the Smart Gate Driver can make sure the correct voltage bias is applied to the gate of the predriver switch and the switch is in the saturation region for the duration of the Miller charging period.



Because the gate of the external MOSFET appears as a short (AC voltage applied to a capacitance) the source or sink current is limited to the saturation current of the switch.

By using multiple switches (shown in Figure 2-2), the Smart Gate Driver can alternate between different current levels during normal operation.

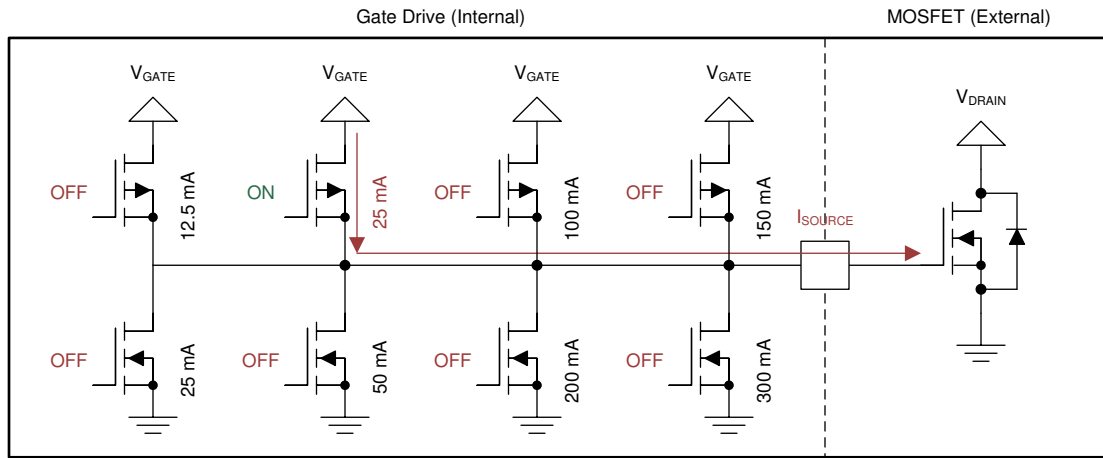


**Figure 2-2. Multiple IDRIVE Settings**

The second method to implement the IDRIVE feature uses current sources instead of switches. This implementation occurs in applications that require very precise and consistent control of the external MOSFET  $V_{DS}$  slew rate across device, voltage, and temperature. While a switch in saturation can be sized appropriately to act as a simple current source, a variation still exists across the previously described factors. To remove this variation, a current source is used in place of the switch (see Figure 2-3). This architecture is especially important in applications that are EMI sensitive and depend on characterizing the system at a specific slew rate.

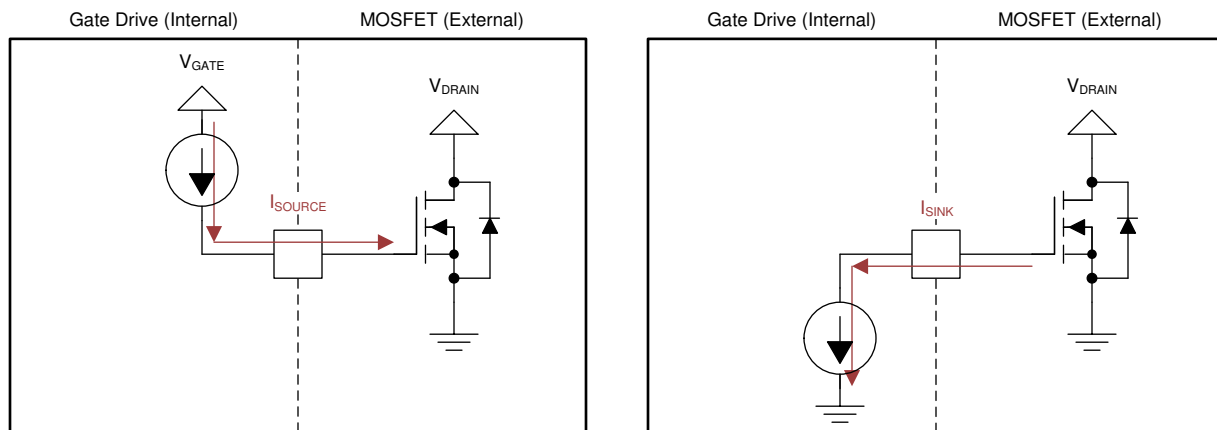


**Figure 2-3. Current Source IDRIVE Method**

Similar to the switch method (Figure 2-2), multiple current sources can be used to provide adjustable gate drive levels.

### 2.1.3 $I_{DRIVE}$ Slew Rate Control

The  $I_{DRIVE}$  feature lets the  $V_{DS}$  slew rate to be adjusted at any time without adding or removing external components to the system. This capability lets a system designer fine tune the switching performance of the MOSFET with regards to efficiency, radiated emissions performance, diode recovery inductive spikes, and  $dV/dt$  turnon.

The persistence plot below shows the effect on the  $V_{DS}$  slew rate from adjusting the  $I_{DRIVE}$  setting on a TI Smart Gate Driver. The MOSFET  $V_{DS}$  is slewing from 24 V to 0 V and the slew rate decreases as  $I_{DRIVE}$  is adjusted across seven levels (10 mA, 20 mA, 30 mA, 40 mA, 50 mA, 60 mA, and 70 mA) of gate source current.

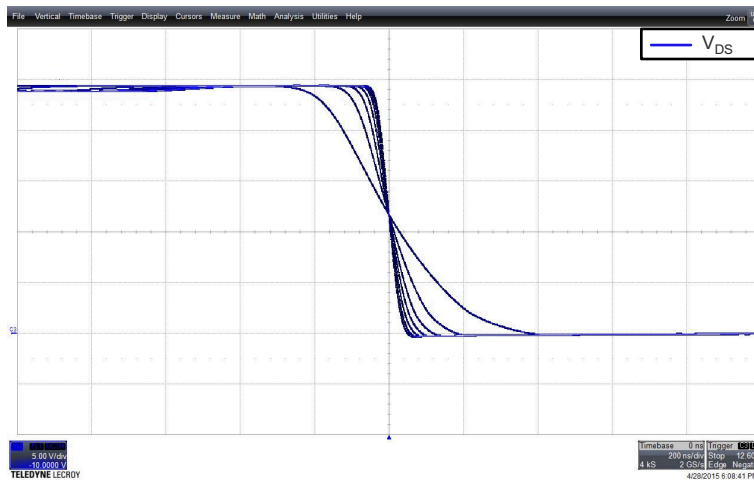


**Figure 2-4.  $V_{DS}$  Persistence Plot Across  $I_{DRIVE}$  Settings**

The following figures show additional signals of the MOSFET while it is being enhanced. The current from the Smart Gate Driver and the Miller region of the external MOSFET is clearly shown when the  $V_{DS}$  slews.

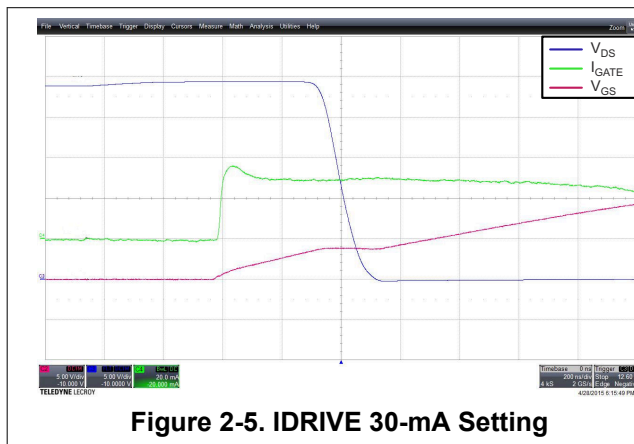


**Figure 2-5.  $I_{DRIVE}$  30-mA Setting**

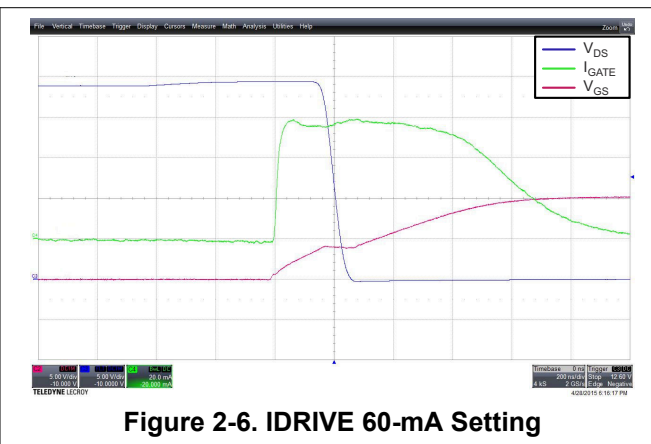


**Figure 2-6.  $I_{DRIVE}$  60-mA Setting**

As mentioned in [Section 1.4](#), if a close-to-ideal current source and an accurate MOSFET  $Q_{GD}$  parameter are available, an approximate calculation for the  $V_{DS}$  slew rate can be made. In the table below, the calculated  $V_{DS}$  slew rate is compared to the measured  $V_{DS}$  slew rate for several  $I_{DRIVE}$  settings. In these calculations, assume that the effects of the series gate resistance and additional non-idealities are minimal.

$$t_{SLEW} = Q_{GD} / I_{SOURCE} \quad (9)$$

**Table 2-1.  $I_{DRIVE}$  Slew-Rate Correlation**

MOSFET $Q_{GD}$ Typical (nC)	$I_{DRIVE}$ Setting (mA)	Calculated Slew Rate (ns)	Measured Slew Rate (ns)	Approximate Error (%)
8	10	800	617	23
8	20	400	305	24
8	30	267	206	23
8	40	200	158	21
8	50	160	128	20
8	60	133	109	18
8	70	114	97	15

Although some error exists from the ideal calculation, these values let a system designer design for an approximate slew rate and then finely tune the system during prototyping. The accuracy of the MOSFET  $Q_{GD}$  plays a large part in the accuracy of the calculation.

The following scope plots are for the different  $I_{DRIVE}$  values shown in the table above.

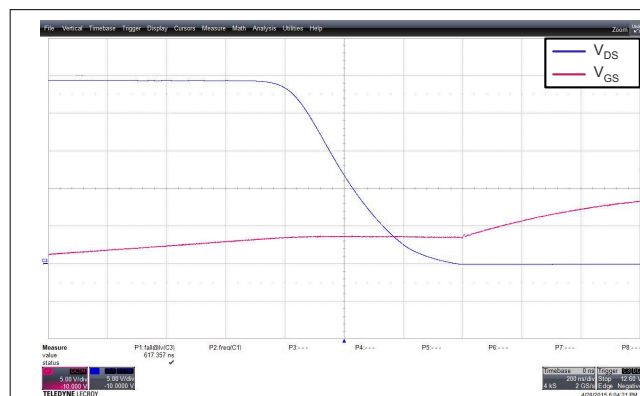


Figure 2-7. 10-mA  $I_{DRIVE}$

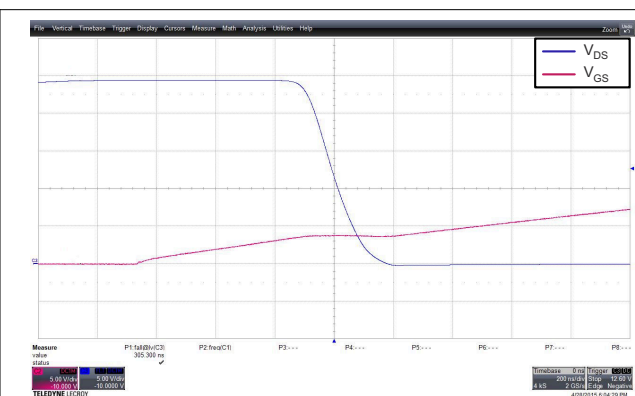


Figure 2-8. 20-mA  $I_{DRIVE}$



Figure 2-9. 30-mA  $I_{DRIVE}$



Figure 2-10. 40-mA  $I_{DRIVE}$



Figure 2-11. 50-mA  $I_{DRIVE}$



Figure 2-12. 60-mA  $I_{DRIVE}$

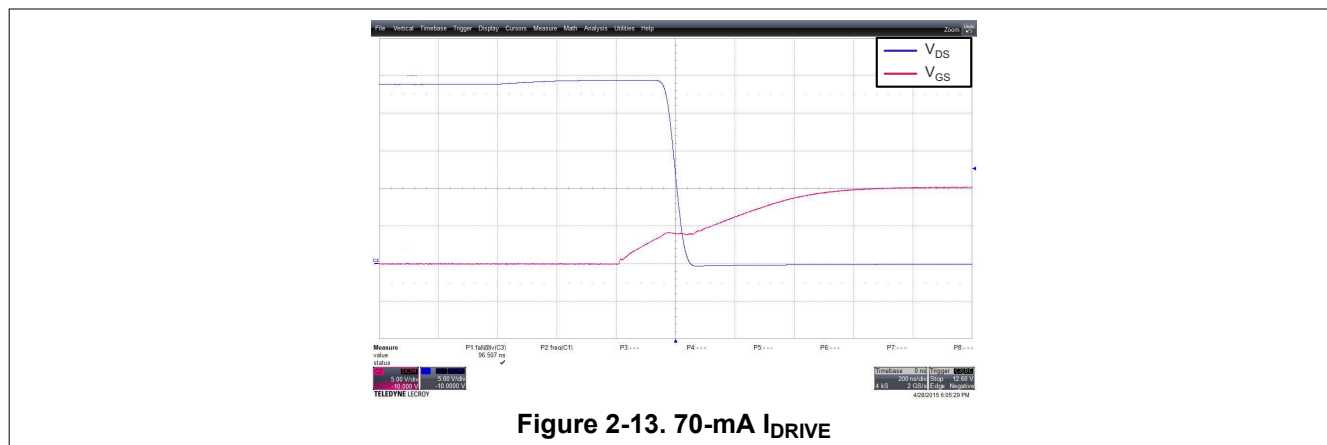


Figure 2-13. 70-mA  $I_{DRIVE}$

### 2.1.4 EMI Optimization Example

One of the leading contributors to electromagnetic interference, also known as EMI, is high frequency noise from the switching of the power MOSFETs. Ideally the square-voltage waveforms generated by the power stage are clean ground-to-supply signals, but this is seldom the case. Parasitics in the MOSFET package and PCB layout can cause undershoot and overshoot voltages that can ring on the switching output. This parasitic ringing can occur at frequencies much greater than 1 MHz, often directly in sensitive spectrum bands. Additionally, the fundamental edge rate of the MOSFET switching can translate into noise in the high frequency spectrum.

While these parasitics can be tackled with layout improvements, snubbers, and design enhancements, often the key knob to tune is the switching speed of the power MOSFETs.  $I_{DRIVE}$  provides an ideal way to tune the motor gate drive system by providing simple control of the MOSFET slew rate through either a register write or one resistor setting which lets system designers select the optimal setting that minimizes efficiency losses while keeping an acceptable EMI level.

The data listed in Table 2-2 is an example from an actual application of the Smart Gate Driver  $I_{DRIVE}$  feature. Table 2-2 shows the peak readings from a CISPR 25 EMI engineering scan from 30 to 200 MHz with a Smart Gate Driver at different  $I_{DRIVE}$  settings. As the  $I_{DRIVE}$  current setting is decreased, the peak scan readings are also decreased.

Table 2-2. EMI Scan Results

$I_{DRIVE}$ Setting (mA)	35-MHz Peak (dB $\mu$ V/m)	65-MHz Peak (dB $\mu$ V/m)	160-MHz Peak (dB $\mu$ V/m)
10/20	5	<0	<0
20/40	12	<0	<0
50/100	12	<0	<0
200/400	28	12	2
250/500	30	15	5

Analyzing the output waveforms on an oscilloscope, it can be seen that at the higher  $I_{DRIVE}$  settings, a high-frequency oscillation is induced on the switch-node. Figure 2-14 shows the high-level oscilloscope capture where the oscillation is not obvious, but by zooming into the end of the rising edge (Figure 2-15) the 35-MHz signal that is in the EMI scans is shown. By reducing the  $I_{DRIVE}$ , the oscillation is almost completely removed (Figure 2-16) which gives an example of how the  $I_{DRIVE}$  architecture would be used in a real-world application. Figure 2-17 through Figure 2-21 show the source EMI scans with the entire 30- to 200-MHz spectrum.

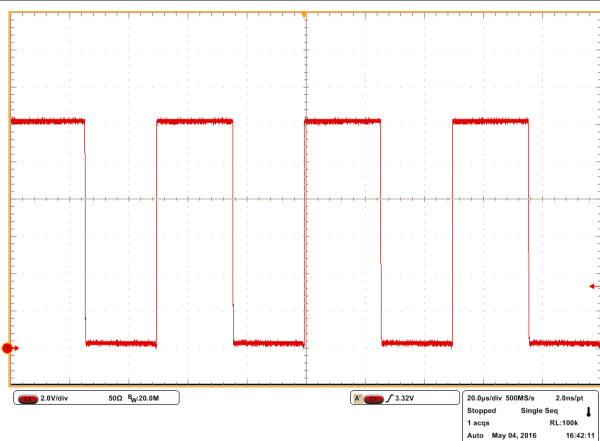


**Figure 2-14. 250/500-mA Switch-Node Waveform**

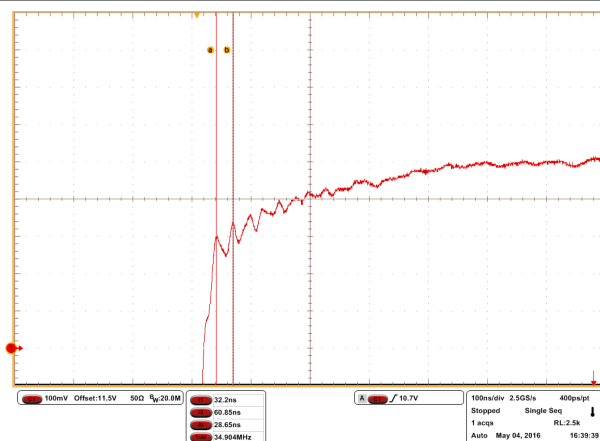


**Figure 2-15. 250/500-mA Switch-Node Waveform Zoom**

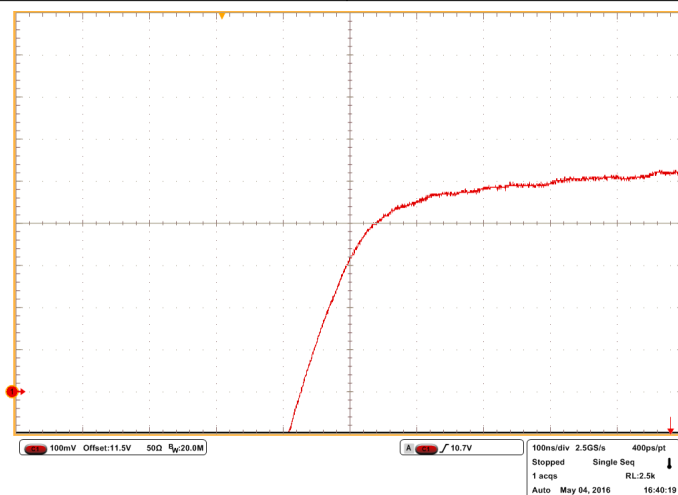


**Figure 2-16. 10/20-mA Switch-Node Waveform Zoom**

Figure 2-17 through Figure 2-21 show the results from the radiated emissions engineering scans for each of the IDRIVE settings.

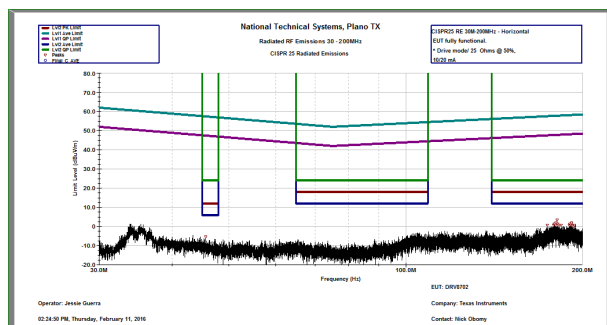


**Figure 2-17. 10/20-mA EMI Scan**

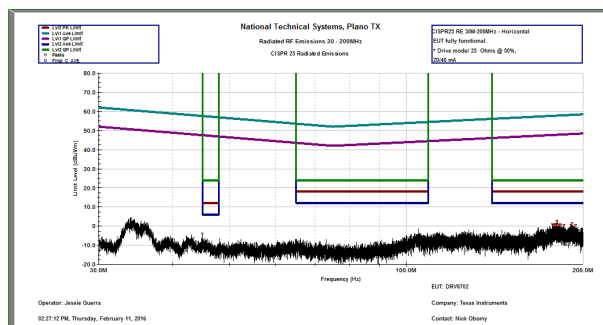


**Figure 2-18. 20/40-mA EMI Scan**

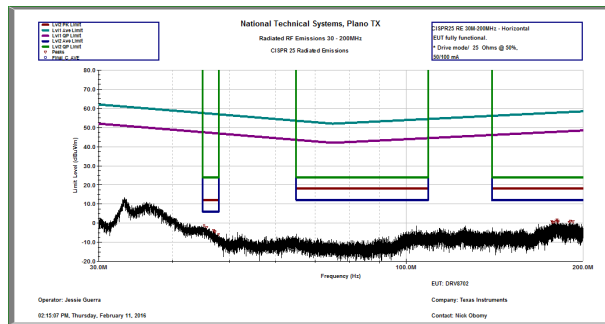


Figure 2-19. 50/100-mA EMI Scan

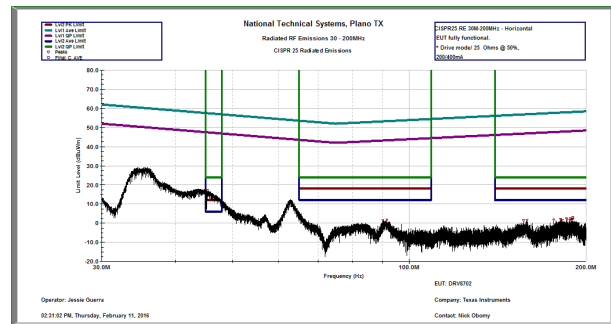


Figure 2-20. 200/400-mA EMI Scan

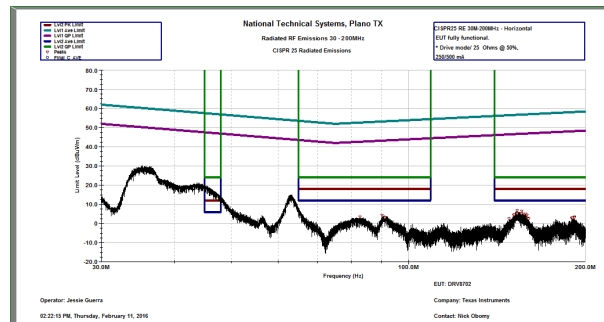


Figure 2-21. 250/500-mA EMI Scan

### 2.1.5 Slew Time Control

On certain TI Smart Gate Drivers, such as DRV8718-Q1 and DRV8714-Q1, an advanced function is provided to regulate the switch-node slew time with closed loop feedback. While open loop control methods described earlier are often sufficient for MOSFET slew rate control, occasionally tighter control is required by the system.

This is due to the fact that key MOSFET parameters can still vary due to manufacturing and system condition variances. Parameters such as the MOSFET gate charge will vary from device to device and even on the same device, changes in the system voltage and temperature will cause these parameters to shift during operation.

In order to solve this challenge a closed loop slew time control loop is required. Closed loop slew time control works by monitoring the switch-node slew time and adjusting the  $I_{DRIVE}$  current setting continuously during operation of the driver in order to achieve a configured target setting. An example of this is shown in the diagram below.

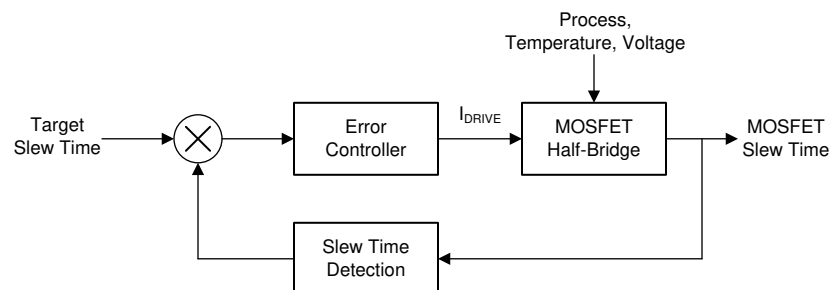


Figure 2-22. Slew Time Control Loop

## 2.2 Robust MOSFET Switching Through $T_{DRIVE}$ State Machine

This section describes some of the common challenges encountered in ensuring robust switching operation and the different features implemented in TI Smart Gate Drivers to solve these challenges.

## 2.2.1 MOSFET Handshaking

In switching MOSFET systems, it is critical to avoid cross-conduction or "shoot-through" conditions to prevent damaging the power MOSFETs or system supply. Cross conduction (shown in [Figure 2-23](#)) occurs when both the high-side and low-side MOSFET are enabled at the same time. A low impedance path is introduced between the power supply and ground. The path lets large current flow, potentially damaging the external MOSFETs or power supply.

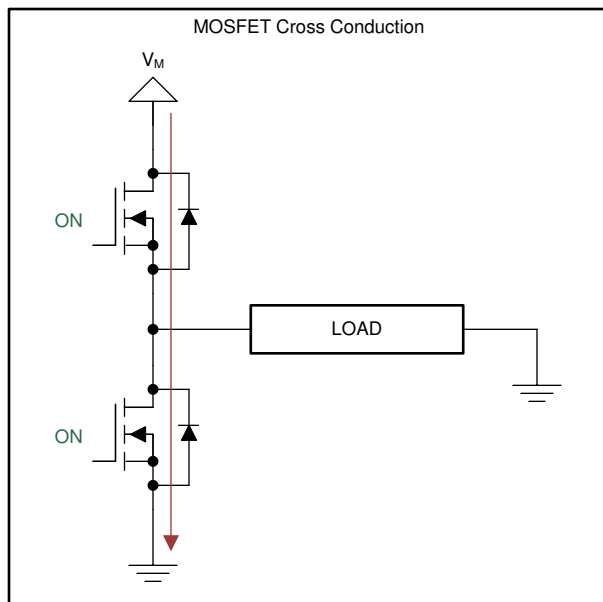


**Figure 2-23. Cross Conduction Example**

Cross conduction, or shoot-through, most commonly occurs when switching from the low-side to high-side (or high-side to low-side). A delay occurs from when the input signal is received to when the external MOSFET is off related to the internal propagation delay and slew rate of the MOSFET. If the opposite MOSFET is enabled before this delay period expires, cross conduction can occur. A simple method to prevent this issue is to add a period of timing before enabling the opposite MOSFET (shown in [Figure 2-24](#)). This period of time is called dead time. Increased dead time decreases the efficiency of the motor driver because of diode conduction losses.

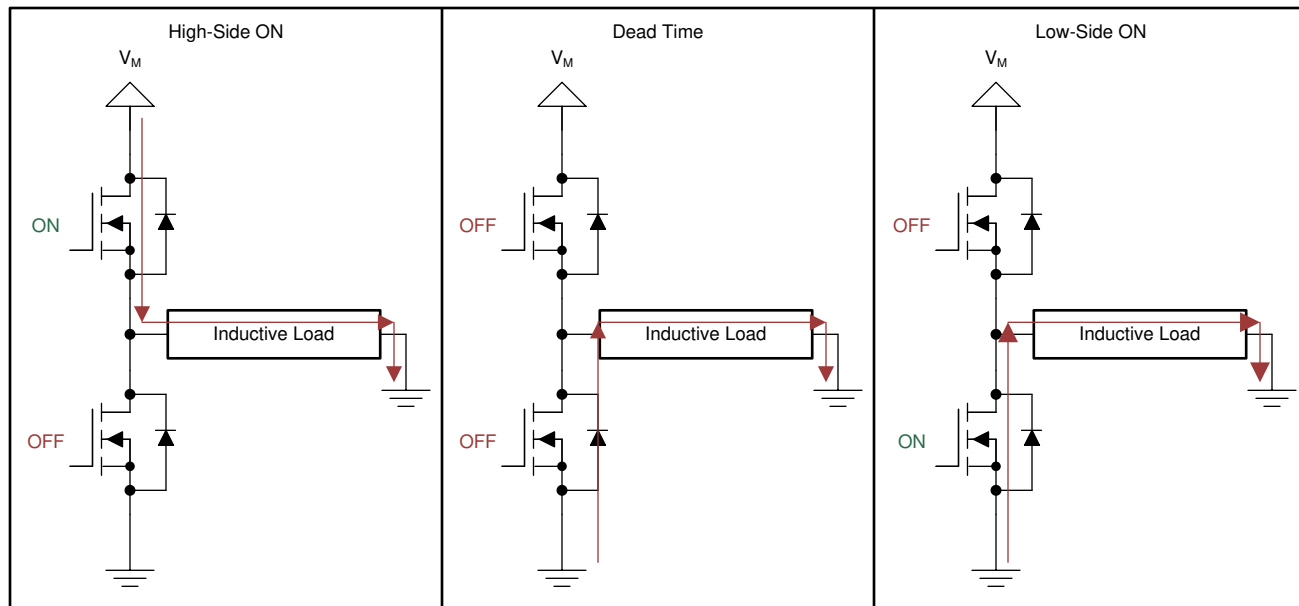


**Figure 2-24. Dead Time Example**

TI Smart Gate Drivers, by monitoring the MOSFET  $V_{GS}$  voltage and with an intelligent  $T_{DRIVE}$  state machine, can provide an optimized amount of dead time for the switching MOSFET system. The  $V_{GS}$  monitors make sure the opposite MOSFET in the half-bridge is disabled before enabling the commanded MOSFET.

In addition to cross conduction protection (shoot-through), this method can provide system performance benefits by reducing the period of diode conduction. Conduction losses of the MOSFET internal body diode are typically worse than standard MOSFET conduction losses and decrease the overall system efficiency.

The  $T_{DRIVE}$  state machine incorporates internal handshaking when switching from the low-side to high-side (or high-side to low-side) external MOSFET. The handshaking is designed to prevent the external MOSFETs from going to a period of cross conduction, also known as shoot-through.

The internal handshaking uses  $V_{GS}$  monitors of the external MOSFETs (Figure 2-25) to determine when one MOSFET has been disabled and the other can be enabled. This handshaking lets the system insert an optimized dead time into the system without the risk of cross conduction.

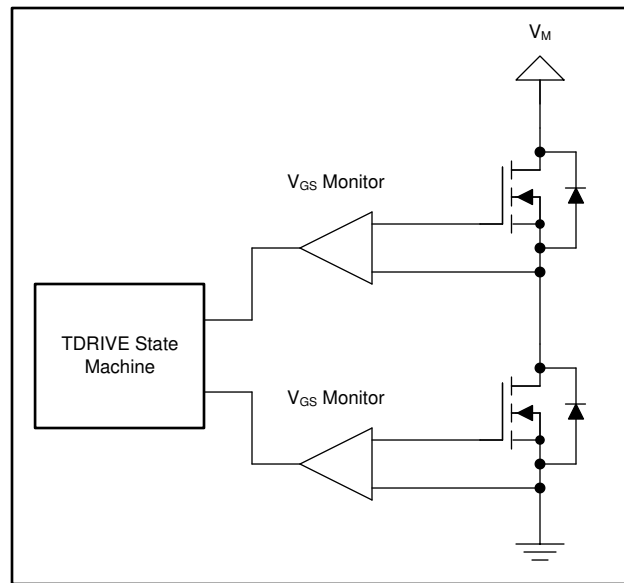


**Figure 2-25.  $V_{GS}$  Monitor Example**

### 2.2.2 MOSFET Gate-Fault Detection

The  $T_{DRIVE}$  state machine lets the Smart Gate Driver detect fault conditions, such as a stuck low or stuck high condition, on the gate of the external MOSFET. Gate faults could be caused by a defect or failure in the power MOSFET gate oxide or a pin fault failure on the gate driver itself. By monitoring the voltage and managing the current to the external power MOSFET, the Smart Gate Driver can detect and report when an abnormal event (partial short, short circuit) has occurred on the MOSFET gate.

The  $T_{DRIVE}$  gate drive timer makes sure that under abnormal circumstances, such as a short on the MOSFET gate or the inadvertent turning on of a MOSFET  $V_{GS}$  clamp, the high peak current through the Smart Gate Driver and MOSFET gate is limited to a fixed duration. Figure 2-26 shows this concept which is outlined as follows:

1. The Smart Gate Driver receives a command to enable the MOSFET gate.
2. A strong current source is then applied to the external MOSFET gate and the gate voltage starts to rise.
3. If the gate voltage has not increased after the  $t_{DRIVE}$  period (indicating a short circuit or overcurrent condition on the MOSFET gate), the Smart Gate Driver signals a gate drive fault and the gate drive is disabled to protect the external MOSFET and gate driver.
4. If a gate drive fault does not occur, the Smart Gate Driver enables a small current source after the  $T_{DRIVE}$  period to keep the correct gate voltage and decrease internal current consumption.



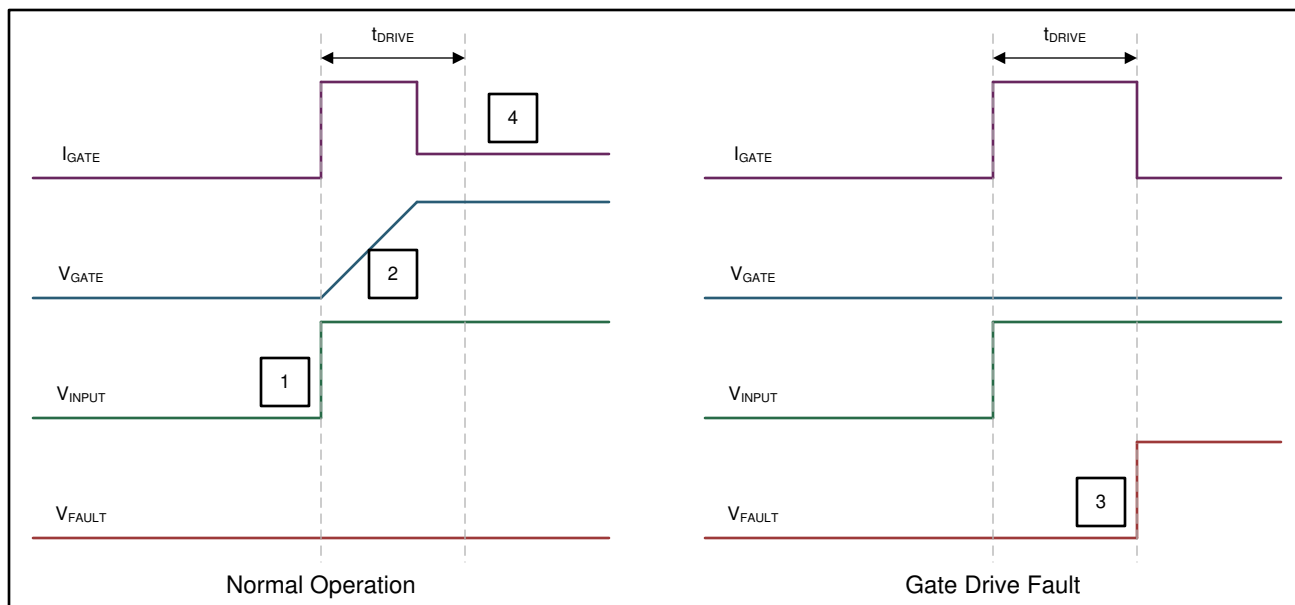


Figure 2-26. TDRIVE Example

### 2.2.3 dV/dt Turnon Prevention

In addition to the cross conduction and gate fault protection features, the internal  $T_{DRIVE}$  state machine also provides a mechanism for preventing dV/dt turnon.

A dV/dt turnon is a system issue that can occur when rapidly slewing the high-side MOSFET. When the switch node rapidly slews from low to high (Figure 2-27), it can couple into the gate of the low-side MOSFET through the parasitic gate-to-drain capacitance ( $C_{GD}$ ). The coupling can raise the gate-to-source voltage of the low-side MOSFET and enable the MOSFET if the voltage crosses the MOSFET threshold voltage ( $V_{th}$ ). If the low-side MOSFET enables while the high-side MOSFET is on, cross conduction occurs.

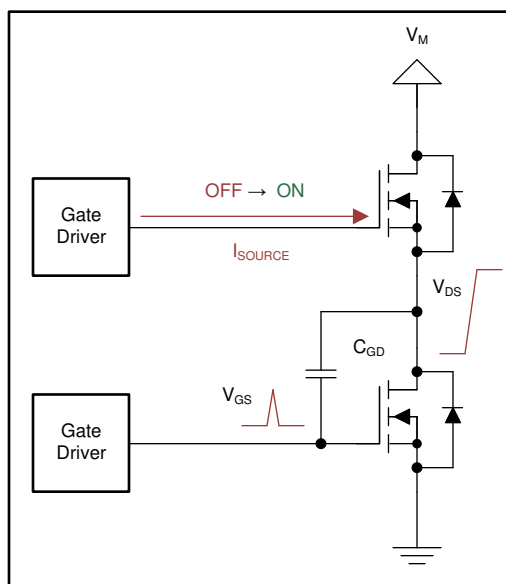
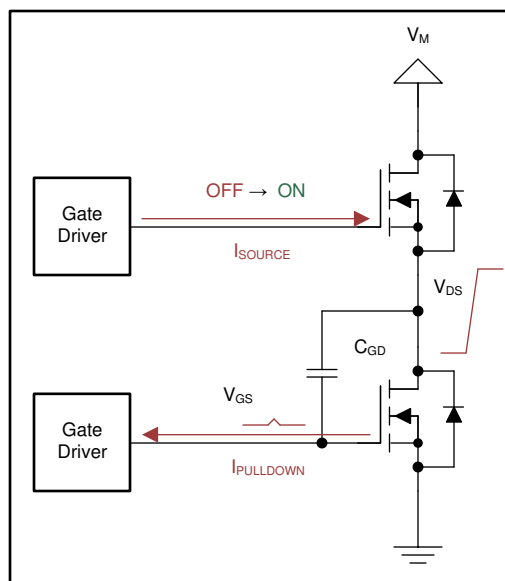


Figure 2-27. dV/dt Example

The  $T_{DRIVE}$  state machine works to prevent dV/dt turnon which can lead to cross conduction in the external half-bridge. By enabling a strong pulldown on the low-side MOSFET during high-side  $V_{DS}$  slew, the Smart Gate Driver can provide a low-impedance path (Figure 2-28) for parasitic charge that couples through the parasitic capacitance of the low-side MOSFET gate to drain capacitance ( $C_{GD}$ ). This impedance path prevents a rise

in the gate-to-source voltage of the low-side MOSFET, which could potentially enable the MOSFET while it is supposed to be off.

The TDRIVE state machine disables the strong pulldown after the switching period and moves to a weak pulldown to decrease the chance of damage to the Smart Gate Driver or system in the scenario of a gate-to-drain short of the external low-side MOSFET. By limiting the period of high current, the Smart Gate Driver can prevent damage to itself and limit further damage to the system.



**Figure 2-28. TDRIVE Pulldown**

## 2.3 System BOM Reduction

In addition to system flexibility, a Smart Gate Driver provides the ability to decrease the system BOM and required board area through integration of key components of the motor gate drive system. A typical Smart Gate Driver block diagram is shown in [Figure 2-29](#).

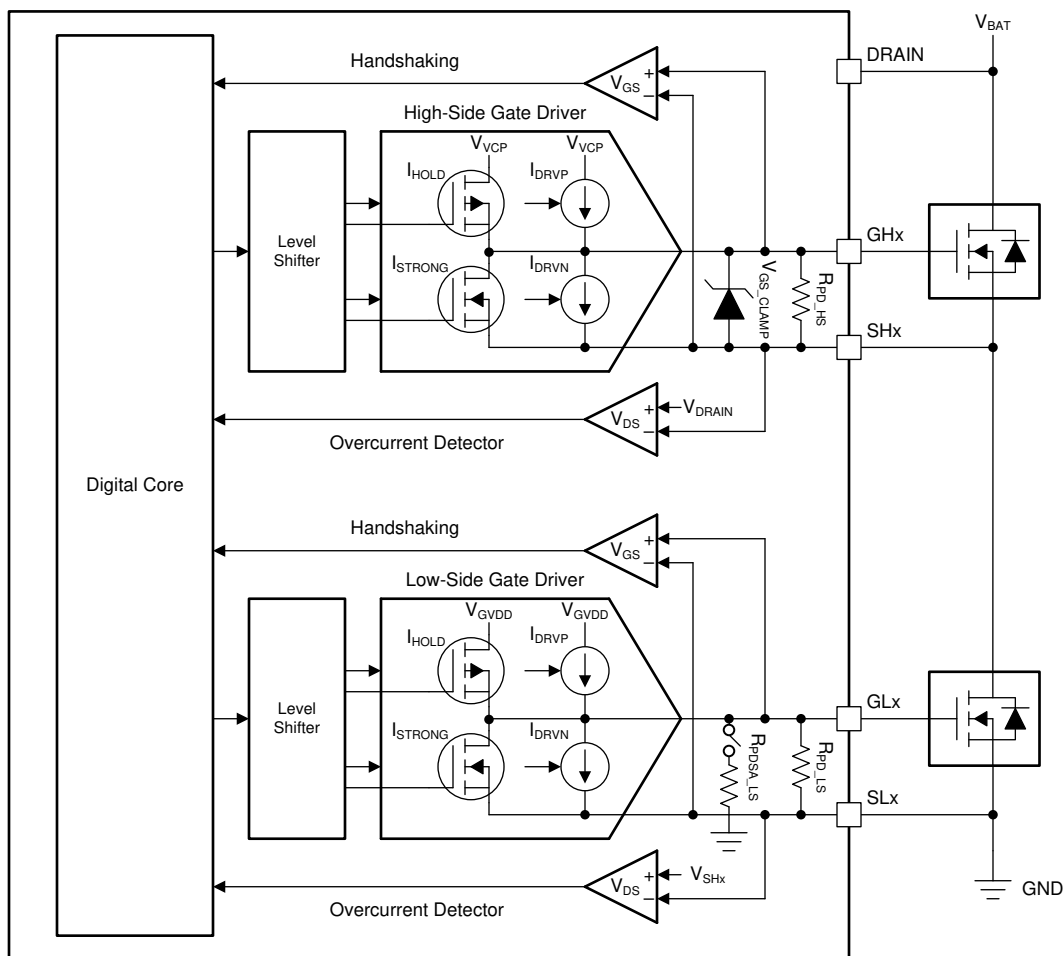


**Figure 2-29. Smart Gate Driver Block Diagram**

The first key point to note is the adjustable gate drive current sources for the turn on and turn off control of the external MOSFET. These are adjustable in order to provide the typical slew rate control compensation that would be done with external components as shown in [Figure 2-30](#). Typically, the  $R_{SOURCE}$  and  $R_{SINK}$  resistors manually adjust the impedance between the gate driver and MOSFET gate. The diode lets the rise and fall  $V_{DS}$  slew rates to be individually adjusted. In a Smart Gate Driver, the adjustable gate drivers integrate this functionality.

Additionally, the internal pull down resistors replace typical external resistors to implement this functionality. The  $R_{PULLDOWN}$  resistor makes sure that the MOSFET stays disabled even when the gate driver is inactive.

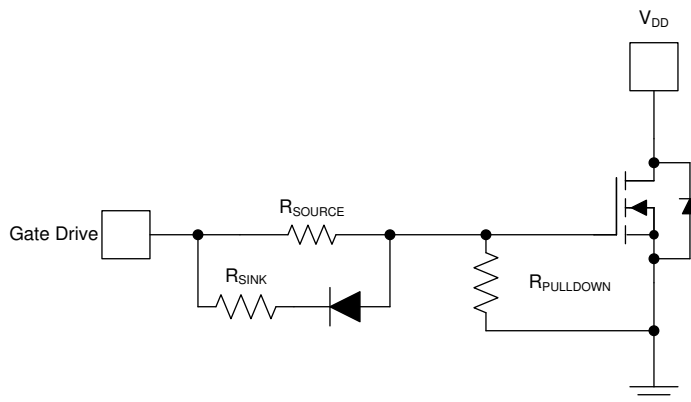


**Figure 2-30. Typical Gate Driver Slew Rate External Components**

Lastly, integrated  $V_{DS}$  and  $V_{GS}$  comparators are provided for every gate driver output. These comparators manage the overcurrent detection for the external MOSFETs and detect potential gate drive faults. These comparators and their various settings can be configured directly through the Smart Gate Driver SPI or hardware settings.

## 2.4 Propagation Delay Optimization

This sections describes some of the common challenges encountered in propagation delay optimization and the different features implemented in TI Smart Gate Drivers to solve these challenges.

### 2.4.1 System Challenges

Another common challenge in motor gate driver system design is managing propagation delay and its impact to the switching performance of the system. Propagation delay has two key parameters that impact overall switching performance. The first is the overall delay from input to out and the second is the mismatch from turn on to turn off. These two parameters will directly impact the minimum and maximum duty cycle, frequency range, and duty cycle step resolution. Good switching performance is important to achieve optimal performance from the motor in regards to speed and torque control.

While most gate drivers will specify their delay and mismatch parameters, they are only one part of the overall input to output system. The other key part is the MOSFET switching delay itself. At high slew rates, the MOSFET contribution to propagation delay and mismatch will often be minimal as compared to the driver, but at slow slew rates, as often found in EMC sensitive systems, the MOSFET can be a main contributor.

Looking further at a typical MOSFET datasheet, we can begin to understand how the MOSFET parameters impact the overall propagation delay. The capacitance parameters across voltage for the CSD18532Q5B are shown below in Figure 2-31.

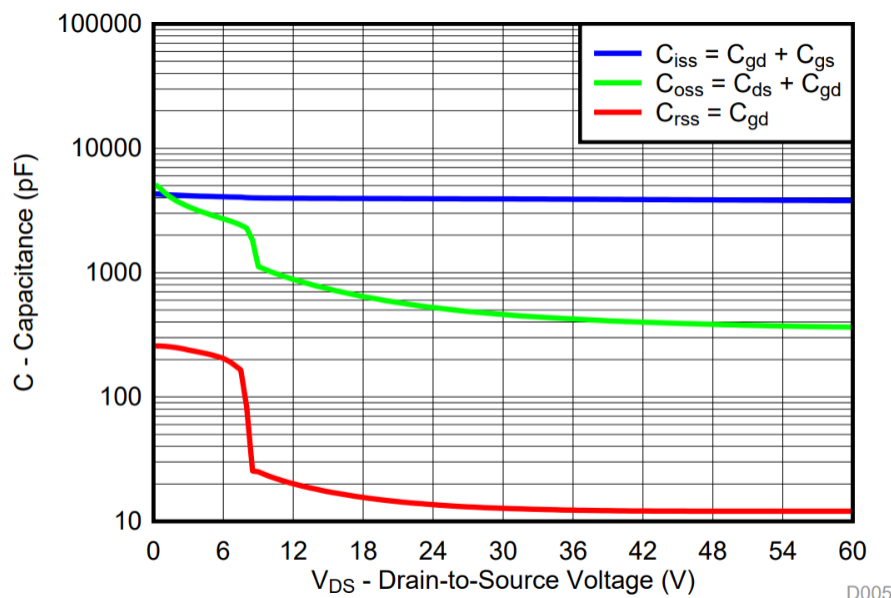


**Figure 2-31. CSD18532Q5B Capacitance Curves**

It is important to understand how these parameters change over voltage as it can be used to determine both the  $Q_{GD}$  and  $Q_{GS}$  of the MOSFET. Oftentimes the  $Q_{GD}$  and  $Q_{GS}$  will be specified as an electrical characteristic of the MOSFET, but this is typically specified at a given  $V_{DS}$  which may not be representative of the actual system conditions.

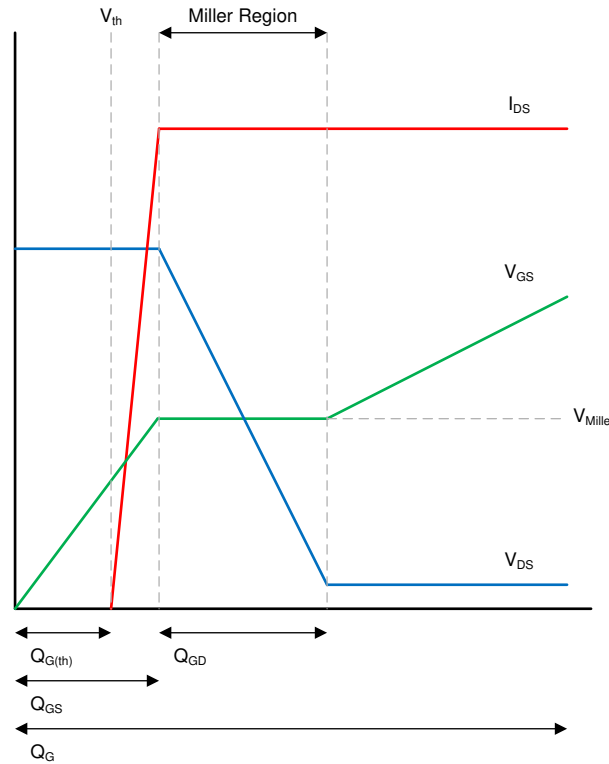


**Figure 2-32. MOSFET Turnon Response**

Referring to the equations below, we can determine a more accurate  $Q_{GD}$  value as a function of  $C_{rss}$  and  $V_{DS}$ . This is integrated over  $V_{DS}$  as this is dynamically changing during the  $Q_{GD}$  charging as shown in [Figure 2-32](#). We can then find a more accurate  $Q_{GS}$  as a function of  $C_{iss}$  and  $V_{DS}$ . This is multiplied as  $V_{DS}$  is relatively static during the  $Q_{GS}$  charging as shown in [Figure 2-32](#).

$$Q_{GD} = \int_0^{V_{DS}} C_{rss} dV \quad Q_{GS} = C_{iss} V_{DS}$$

**Figure 2-33. Charge Calculations**

From  $Q_{GD}$  and  $Q_{GS}$  we can determine the MOSFET contribution to propagation delay and slew time.

$$t_{prop} = \frac{Q_{GS}}{I_{Source}} \quad t_{slew} = \frac{Q_{GD}}{I_{Source}}$$

**Figure 2-34. Timing Calculations**

Using the CSD18532Q5B MOSFET example again, we can calculate an approximate  $Q_{GD}$  and  $Q_{GS}$ . Assuming a 12 V power supply,  $Q_{GD}$  is approximately 1.2 nC and  $Q_{GS}$  is approximately 6.9 nC. Further assuming a 1us slew time, we can calculate an  $I_{Source}$  of 1.2 mA. From this, we can calculate the approximate propagation delay to be 5.75 us. In summary, we can see that  $Q_{GS} \gg Q_{GD}$  and this typically holds true for most MOSFETs. We can also conclude that at slower slew rates the propagation delay time becomes a significant factor in switching performance. If using a 20kHz PWM signal, a greater than 5 us propagation delay is already more than 10% of the overall period.

## 2.4.2 Propagation Delay Reduction

On certain TI Smart Gate Drivers, such as DRV8718-Q1 and DRV8714-Q1, an advanced function is provided to reduce the propagation delay for the MOSFET charge and discharge by using a dynamic current control

scheme. This scheme reduces propagation delay in order to support a wider PWM duty cycle range and also to reduce thermal dissipation in the MOSFET as it moves through the residual charging region after the miller charge region. This is shown in Figure 2-35 and Figure 2-36. The dynamic current control has several regions including a pre-charge current ( $I_{PRE\_CHR}$ ) for reducing propagation delay ( $t_{DON/OFF}$ ), a drive current ( $I_{DRVP/N}$ ) for slew rate control, and a post-charge current ( $I_{PST\_CHR}$ ) for residual charging.

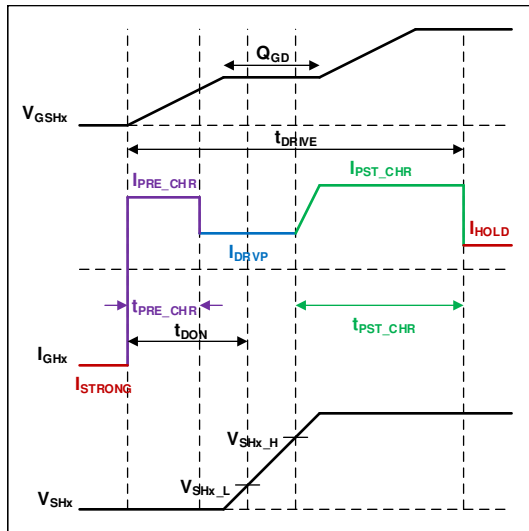


Figure 2-35. Dynamic Pre-Charge Profile

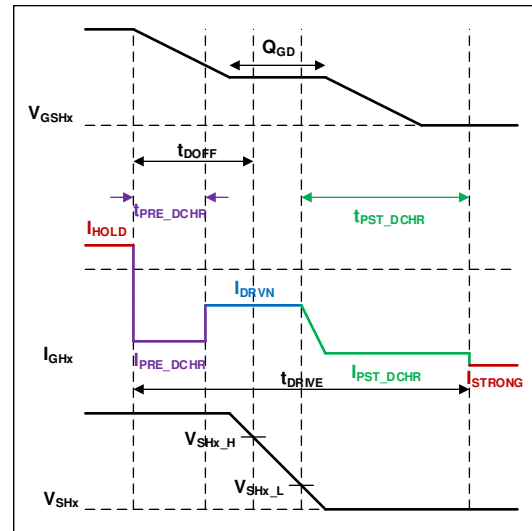


Figure 2-36. Dynamic Post-Charge Profile

In order to implement robust dynamic current control, the Smart Gate Driver uses an adaptive scheme to learn and predict when the switch node is going to enter the slewing region and preemptively adjust the gate drive current. A predictive scheme is required as the typical delays from using direct feedback with comparators could impact the slewing region itself.

In this adaptive scheme, the controller modulates the current for a proportion of the programmed propagation delay and then monitors at which point the switch-node slews. Based on whether the switch-node slews early or late the pre-charge current is then adjusted up or down as shown in Figure 2-37. Every PWM cycle, the pre-charge current ( $I_{PRE\_CHR}$ ) is updated based on the switch-node ( $V_{SH}$ ) slew timing until the desired propagation delay ( $t_{DON}$ ) is reached.

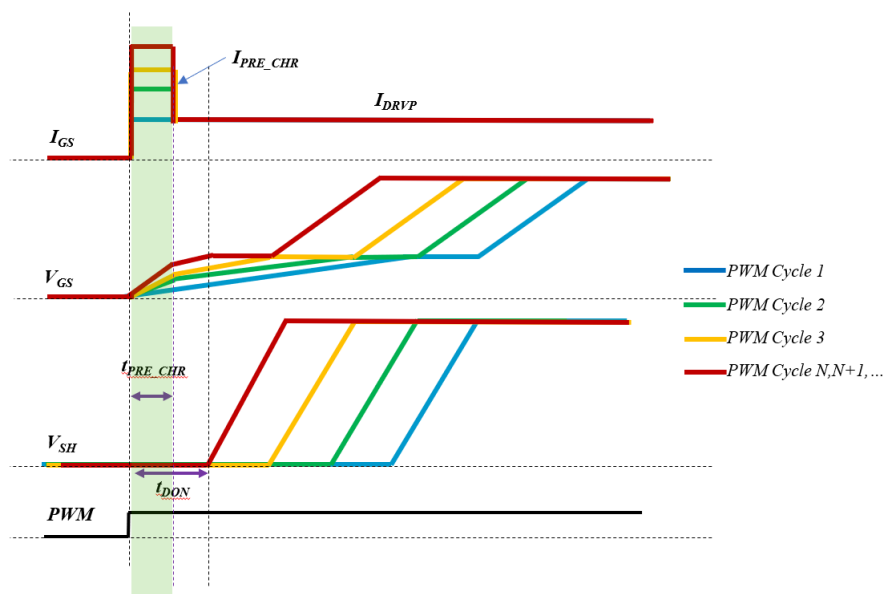


Figure 2-37. Propagation Delay Adaptive Adjustment

### 3 Revision History

NOTE: Page numbers for previous revisions may differ from page numbers in the current version.

<b>Changes from Revision C (November 2018) to Revision D (March 2021)</b>	<b>Page</b>
• Updated abstract.....	<a href="#">1</a>
• Combined Smart Gate Driver Features and System Benefits sections to improve organization.....	<a href="#">8</a>
• Added Slew Time Control section.....	<a href="#">14</a>
• Added Propation Delay Optimization section.....	<a href="#">21</a>
<b>Changes from Revision B (January 2018) to Revision C (November 2018)</b>	<b>Page</b>
• Changed spec values in <a href="#">Table 1-1</a> .....	<a href="#">3</a>
• Changed "6.9 nC" to "44 nC" in <a href="#">Section 1.5.2</a> .....	<a href="#">7</a>
<b>Changes from Revision A (May 2016) to Revision B (January 2017)</b>	<b>Page</b>
• Updated terminology to Smart Gate Driver.....	<a href="#">1</a>

## IMPORTANT NOTICE AND DISCLAIMER

TI PROVIDES TECHNICAL AND RELIABILITY DATA (INCLUDING DATA SHEETS), DESIGN RESOURCES (INCLUDING REFERENCE DESIGNS), APPLICATION OR OTHER DESIGN ADVICE, WEB TOOLS, SAFETY INFORMATION, AND OTHER RESOURCES "AS IS" AND WITH ALL FAULTS, AND DISCLAIMS ALL WARRANTIES, EXPRESS AND IMPLIED, INCLUDING WITHOUT LIMITATION ANY IMPLIED WARRANTIES OF MERCHANTABILITY, FITNESS FOR A PARTICULAR PURPOSE OR NON-INFRINGEMENT OF THIRD PARTY INTELLECTUAL PROPERTY RIGHTS.

These resources are intended for skilled developers designing with TI products. You are solely responsible for (1) selecting the appropriate TI products for your application, (2) designing, validating and testing your application, and (3) ensuring your application meets applicable standards, and any other safety, security, regulatory or other requirements.

These resources are subject to change without notice. TI grants you permission to use these resources only for development of an application that uses the TI products described in the resource. Other reproduction and display of these resources is prohibited. No license is granted to any other TI intellectual property right or to any third party intellectual property right. TI disclaims responsibility for, and you will fully indemnify TI and its representatives against, any claims, damages, costs, losses, and liabilities arising out of your use of these resources.

TI's products are provided subject to [TI's Terms of Sale](#) or other applicable terms available either on [ti.com](#) or provided in conjunction with such TI products. TI's provision of these resources does not expand or otherwise alter TI's applicable warranties or warranty disclaimers for TI products.

TI objects to and rejects any additional or different terms you may have proposed.

Mailing Address: Texas Instruments, Post Office Box 655303, Dallas, Texas 75265  
Copyright © 2022, Texas Instruments Incorporated